

SABRAO Journal of Breeding and Genetics  
 56 (1) 353-369, 2024  
<http://doi.org/10.54910/sabrao2024.56.1.32>  
<http://sabraojournal.org/>  
 pISSN 1029-7073; eISSN 2224-8978



## LOW-COST SOIL MOISTURE SENSORS' ASSESSMENT FOR THEIR ACCURACY AFTER CALIBRATION THROUGH THE GRAVIMETRIC METHOD

**M.A.M. AL-RAWI**

Department of Soil Sciences and Water Resources, College of Agricultural Engineering Sciences, Baghdad University, Iraq  
 mohammed.alrawi@coagri.uobaghdad.edu.iq

### SUMMARY

The existing study aimed to assess four soil moisture sensors' capacitive (WH51 and SKU: SEN0193) and resistive (YI69 and IC Station) abilities, which are affordable and medium-priced for their accuracy in six common soil types in the central region of Iraq. The readings' calibration for the soil moisture sensor devices continued through two gravimetric methods. The first depended on the protocols' database, while the second was the traditional calibration method. The second method recorded the lowest analysis error compared with the first. The moderate-cost sensor WH51 showed the lowest standard error (SE), MAD, and RMSE and the highest  $R^2$  in both methods. The performance accuracy of WH51 was close to readings shown by the manufacturing company (1%), as the MAD amounted to 1.62%. Through both methods, the average MAD for sensors ranged from 4.76% to 7.36%, with this result considered acceptable, especially for low-cost sensors with insufficient available information for accuracy. In general, the average mean absolute percentage (MAPE) for all sensors was 25.54%, which means that the validity of the measurement for the low-cost sensors reached 75%. It encourages their use by plant breeders in irrigation, as the error rate was less than the specified depletion of 50% for available water in irrigation, where all study textures showed that the sensor reading reached the limits of  $72 (\pm 2)$ , adopting 3% MAD for all sensors. The study affirms that, except for the IC station sensor recommended for irrigation use only in sandy-sandy loam soils, low-cost sensors have suitable accuracy for irrigation management.

**Keywords:** Soil moisture sensors, gravimetric methods, calibration equations, accuracy, MAPE, WH51

**Key findings:** For all the sensors' calibration through both methods, the average MAD ranged from 4.76% to 7.36%, and these results showed considerable acceptance, especially for low-cost sensors. In general, the average mean absolute percentage (MAPE) for all sensors was 25.54%, which authenticates the validity of the measurements for inexpensive sensors (75% or more), encouraging their use in the irrigation field by applying its calibration equation.

Communicating Editor: Prof. Naqib Ullah Khan

Manuscript received: June 7, 2023; Accepted: November 9, 2023.

© Society for the Advancement of Breeding Research in Asia and Oceania (SABRAO) 2024

**Citation:** Al-Rawi MAM (2024). Low-cost soil moisture sensors' assessment for their accuracy after calibration through the gravimetric method. *SABRAO J. Breed. Genet.* 56(1): 353-369. <http://doi.org/10.54910/sabrao2024.56.1.32>.

## INTRODUCTION

Water resources face many threats in Iraq, as large areas dried up and water resources shrank due to the building of new dams to store water in neighboring countries like Syria, Turkey, and Iran (Al-Lami *et al.*, 2023). Such a situation requires using modern methods to manage and reduce the excessive use of water resources and rationalize irrigation water consumption. With insufficient rains, the rivers become the primary sources of irrigation, particularly in Central, Southern, and Western Iraq (Abbas, 2021). All of the above would not be achievable without using available methods to monitor soil moisture in real-time and provide irrigation per the plant's needs; hence, moisture sensors are one of these methods.

The Internet of Things (IoT) is a new area of technology that allows physical objects to communicate with others to make human life better and more convenient (Afifie *et al.*, 2021). The IoT-based moisture sensors have become a basic necessity in chemical, industrial, and agricultural applications. An interest in mobile wireless sensor networks has gained enhancement based on their capability to provide better solutions with low-priced tools in multiple fields (Salman and Alisa, 2019). The moisture sensor is more rapid with an accurate remote-control system and completion of tasks, as well as it checks all the processes by itself.

There are various types of moisture sensors, and their use is complex in solving agriculture's irrigation problems (Bittelli *et al.*, 2008). Campbell *et al.* (2009) defined the moisture sensor as a small and efficient device that works to detect the physical conditions surrounding it, converting the signals falling on it into electrical pulses, i.e., the physical quantities (humidity, temperature, pressure, light, and salinity) into electrical quantities (current-voltage and resistance). Its counting can be through a device, with the intensity of the effects known by connecting it to a computer. In agriculture and irrigation, some networks rely on sensors that measure soil moisture and water levels in reservoirs and are of high economic feasibility in countries suffering from insufficient water and rain.

Well-designed irrigation systems aim to meet crops' water needs by monitoring soil moisture and other environmental parameters. The systems based on IoT record data in the cloud, and the farmer can oversee the water pumps through an Android application (Kagalkar, 2017). The smart irrigation system requires the soil moisture data to determine the soil condition in real-time, with the sensor calibrated before use for quick irrigation. In previous studies, the soil moisture sensor YL-69's calibration utilized the gravimetric water content method, showing the mean absolute error (MAE) of the proposed calibration equations ranged between 2.92%–5.37% (Setyowati *et al.*, 2020). Batllori (2020) found that moisture sensors differed in their response to the volumetric water content (VWC), with the range of VWC for the resistive IC Station sensor only at 0%–15%, while in the capacitive SKU: SEN0193 sensors, the scope was 0%–30% in clay soil and reaching 40% in sand soil.

In soil, the water balance is very complex as it moves in a multi-directional process; even in isotropic soil, the flow does not accurately follow the head gradient because of anisotropy induced by the moisture gradient (Jackson, 1992). Therefore, the plant breeders and farming community need to add irrigation requirements by monitoring the soil moisture with sensors available in the market at different costs, which may be expensive in some regions globally or low-cost in others, according to the purchasing power per capita. The presented study sought to assess the low-cost (according to Iraqi conditions) soil moisture sensors after calibrating them with the gravimetric method, identifying the model that links the relationship between sensor reading and soil water content in a better way, and get the best calibration curve and the closest one to the results of the gravimetric method.

## MATERIALS AND METHODS

The experiment commenced in July 2022 at the region of Al-Amriya, Baghdad Governorate, Iraq at 33° 18' 28.2" N, 44° 17' 55.3" E.

**Table 1.** Soil properties for the experimental treatments.

Position	Symb ol	Texture Class	Sand g/kg	Silt g/kg	Clay g/kg	Org. Mat. %	Wilt. Pt. cm <sup>3</sup> .cm <sup>-3</sup>	Field Cap cm <sup>3</sup> .cm <sup>-3</sup>	Saturation cm <sup>3</sup> .cm <sup>-3</sup>	Available water	Bulk Density g/cc
Abu-Graib Front	AGB	Clay Loam	413	263	324	1.1	0.126	0.365	0.655	0.239	1.34
Garden House - Baghdad	FGHB	Sandy Loam	767	130	103	0.27	0.100	0.136	0.506	0.036	1.58
Garden House - Baghdad	GHB	Sandy Clay Loam	666	125	209	0.25	0.082	0.157	0.516	0.075	1.45
Back Garden House - Baghdad	BGHB	Sandy Clay Loam	641	121	238	0.68	0.106	0.174	0.497	0.068	1.43
Desert Soil- AL- Jabariyah	DSJ	Sandy Loam	661	146	193	6.8	0.178	0.361	0.516	0.183	1.45
River Soil - AL- Jabariyah	RSJ	Sandy Loam	746	99	155	0.5	0.044	0.103	0.495	0.059	1.51

### Soil study

Iraq's division into four agro-environmental regions comprised the irrigated area that extends between the Tigris and Euphrates rivers, the arid and semi-arid regions, the steppes, and the desert regions (Bishay, 2003; Al-Rawi and Bahia, 2020). Soil samples came from six different sites, five representing the irrigated areas and one from the desert area. All the soil types properties are available in Table 1 and are as follows:

**Abu-Graib (AGB):** Clay loam texture soil, classified among the major soil groups (Typic Torrifluvents) according to USDA (1975), and also discussed in past studies (Ahmad *et al.*, 2006; Muhaimed *et al.*, 2014; Al-Rawi, 2017).

**Front Garden House - Baghdad (FGHB):** Sandy loam soil, transported from the levee of the Tigris River for the cultivation of home gardens, taken from the front garden of a residential house in the District Al-Amriya, capital of Baghdad, Iraq, and planted with palm trees and some weeds. Soil Levee Tigris River characteristics described and discussed by Buringh and Edelman (1955), Kukal and Al-

Jassim (1971), Eltaif and Gharaibeh (2022), and Al-Mafrajee and El-Rubae (2022).

**Garden House - Baghdad (GHB):** A sample taken from inside the house with a finer texture than that from the front garden (sandy clay loam), planted with palm trees, citrus fruits, and grass, and also probed in past studies (Al-Rawi and Al-Mashhadani, 2021; Al-Halfi and Al-Azzawi, 2022).

**Back Garden House - Baghdad (BGHB):** Similar to GHB specifications, but uncultivated and showing natural plants.

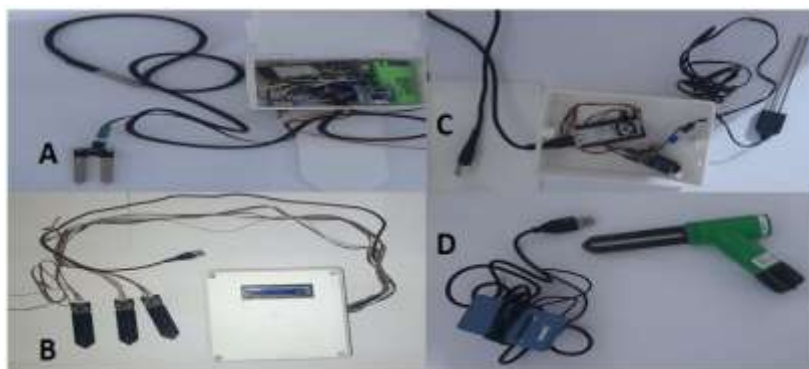
**Desert Soil- AL-Jabariyah (DSJ):** Taken from the western region of Iraq at 34° 26' 24" E latitude and 41° 17' 24" S longitude in the village of Al Jabariyah, lower Al-Jazeera Region, Iraq. More characteristics of this soil are available in the studies of Al-Rawi (2014). It has a sandy loam texture as one of the dominant textures in Iraqi desert regions after loamy sand (Isa and Suliman, 2020). More ecological characteristics and biotope distribution are accessible in the studies of Solijonov and Umarov (2022).

**Table 2.** Categories of used sensors, their models, manufacturer, prices, and costs.

Measurement Technique	Soil Moisture Sensor Company	Price USD	Cost
Resistance	YL69 KitsGuru module	1.8	Very Low cost
Capacitance Based	SKU: SEN0193, Reland-Sung Industrial	8.69	Low cost
Resistance	Soil humidity sensor, Corrosion Resistance Module, IC Station company	7.88	Low cost
Capacitance	ECOWITT GW1106 Soil Moisture Meter, Includes GW1100 Wi-Fi Gateway and WH51 Soil Moisture Sensor, ECOWITT company	54	Moderate cost

**Table 3.** The most important specifications of the soil moisture sensors used in the study.

Soil Moisture Sensor Module	Operating Voltage	Output Voltage	Probe Size	Resolution	Burial Ability
Corrosion IC Station	.3 - 12V	0 - 12V	8.8cm	Non	burial able
YL-69	3.3 - 5V	0 - 5V	6 cm × 2 cm	Non	burial able
SKU: SEN0193	.3 - 5.5V	0 - 3.0V	9.8 cm × 2.3 cm	Non	not burial able
ECOWITT WH51	1.5 V	-----	8 cm × 2 cm	1%	not burial able

**Figure 1:** Soil Moisture Sensors: (A) YL-69 with Temperature Sensor DS18B20, (B) Capacitive soil moisture sensor SKU: SEN0193, (C) Corrosion Resistance Module IC Station, and (D) ECOWITT WH51 Soil Moisture Sensor.

**River Soil - AL-Jabariyah (RSJ):** A sample collected from the Euphrates River Levee in Jabariyah ensued. This Levee extends along the main river channels and river bends; their origins are different, and a summary of their general characteristics consisted of coarse to medium texture from fine sand to silty clay loam, and its construction was weak to medium (Buringh, 1960; Muhaimeed and Muhammad, 2010). A Jabariyah Levee sample is a coarse texture soil (loamy sand to sandy loam) of which sand content may be more than 75% with a little clay content.

### Soil moisture sensors

This study tested four medium- and low-cost moisture sensors, with their costs, producing companies, and information about their specifications provided in Tables 2 and 3.

#### Soil moisture sensor YL-69

This sensor depended on the principle of electrical resistance, consisting of two pieces, the electronic board (right of Figure 1A) and the two-legged probe, which detects the water

content (left of Figure 1A). The sensor receives an electrical circuit connected to the Internet via the Esp8266 model, which works as a Wi-Fi unit, and an added sensor helps measure the ambient temperature (Figure 1A). The code entry for the sensor ran through the Arduino programming. The electrical circuit design and the code for the sensor, the method of connecting the Arduino board, and entering the code are available in Tutorials (2017).

### **Capacitive soil moisture sensor SKU: SEN0193**

A capacitive-based soil moisture sensor visualizes analog voltage variations with changes in water content. In capacitive structures, any measurement affecting the electrode separation distance, electrode overlap area, and the relative dielectric permittivity near the electrodes sustains sensing by observing changes in the structure's capacitance (Mander and Arora, 2014). The characteristics of capacitive sensors differ from other technologies, and with this sensor, there is a method for measuring variations near the surface of the sensor, and the measurements do not have the potential health risks of radiation-based techniques. Soil Moisture Sensor SKU - SEN0193's design includes two parallel plates, with the measured soil between both poles, and acts as a dielectric material for the capacitor, one of the low-cost soil moisture sensors (Figure 1B). The sensor associated with this signal conditioning circuit acquires a connection to the Arduino microcontroller and the LCD of the data acquisition system (Figure 1B). Muzdrikah *et al.* (2018) findings revealed that the soil water content readings by SKU: SEN0193 bore no effects from the differences in soil volume and soil temperature; however, they incur slight influences from the surrounding environmental temperature, showing a direct relationship between soil water content and sensor response. Like other capacitive sensors, it is also distinct in its

ability to reduce the effect of ionic activities that usually occur in cultivated soils.

### **Corrosion resistance module (IC Station)**

A product of the IC Station, it is considerably one of the electrical resistance sensors. The model contains digital and analog outputs and a potentiometer to adjust the threshold level. It is characteristic of being waterproof and highly resistant to rust, with the possibility of being buried and staying inside the soil for not less than six months (IC Station, 2022). It has an interface with a NodeMcu board for Arduino programming applications, including frameworks running on the ESP8266 Wi-Fi SoC (Figure 1C).

### **Soil moisture sensor for climate station ECOWITT WH51**

A capacitive sensor, commonly used in climate stations, sends data to the weather station control unit via Wi-Fi (Ecowitt, 2022a). It also consists of two pieces: the first is a compact installation in the form of a pistol that contains the LED indicator that gives RF transmission and a slot for AA batteries, in addition to the sensor, which is a metal rod. The second is a GW1000 Wi-Fi. When connected to the Internet, the Local Area Network (LAN) receives the RF transmission from the sensor to send to the WS View website, which is available as an application on smartphone devices. This sensor is the most expensive compared with other sensors used in this study (Figure 1D)

### **Data recorded**

All data received for YL-69, SKU: SEN0193, and IC Station sensors occurred via mobile device using the Blynk application (Figure 2), and data gathering for the WH51 sensor (Figure 3) employed the WS View application via mobile from Shenzhen (2022) or PC from Ecowitt (2022b).



**Figure 2.** YL69, IC Station, and SKU: SEN0193 sensor data board via the Blynk app designed to read three sensors of each type and a DS18B20 temperature sensor with a YL69 sensor.



**Figure 3.** ECOWITT WH51 sensor data board via the WS View app.

### Sensor's calibration

The sensors calibration proceeded through the gravimetric method of soil containers using two methods:

#### **Laboratory calibration of repacked soils method**

This first method has details from an online database (Adla *et al.*, 2019) based on the standard calibration procedure suggested by Decagon Devices Inc. (Campbell *et al.*, 2007). This method relied upon using soil from the field and repackaged free of the assemblies in

small containers inside the laboratory. After wetting them with different moisture levels, sensor readings continued at the initial moisture, and after a specific period, other gauges also attained recording indicating the final dampness. The same-sized glass container used (Figure 4A) was broader than the impact size of the soil moisture sensors for calibration but not so big for a tendency to form moisture gradients within the soil. The selected containers were 6 cm in diameter and 9 cm in height. Five containers prepared for each of the six textures of ground comprised the experiment to make a total of 30 containers. An added amount of intermediate



**Figure 4.** (A) Method 1 and (B & C) Method 2 treatments.

mineral concentration tap water (based on EU directive [Van der, 2003]) by 0.8 ds.cm<sup>-1</sup> EC (512 mg.L<sup>-1</sup> TDS) to the fifth container of each group was enough to make the soil saturated, then augmenting followed at 75%, 50%, 25%, and 0% to containers 4, 3, 2, and 1, respectively. The data tabulation used the Template\_Tables.xls file (Adla *et al.*, 2019) containing templates for entering data during the calibration procedure. These templates allowed entering data for container volume, soil weight, and the added water to calculate the bulk density of the sample and extract the actual volumetric water content  $\theta_{act}$  simultaneously with the sensor readings to obtain the calibration curves.  $\theta_{act}$  calculation for each container followed the Equation 1 below:

$$\theta_{act} \% = \frac{\text{Volume of water added [cm}^3]}{\left( \frac{\text{Mass of soil [g]}}{\text{Bulk density of soil } \left[ \frac{\text{g}}{\text{cm}^3} \right]} \right)} \times 100 \quad \text{-----(1)}$$

The readings noted every 30 min after humidification represented the initial moisture, with a final reading taken 24 hours after humidification to denote the endmost moistness. Calculations ensued for the actual volumetric water content (VWC) for the initial moisture content (VWC<sub>int</sub>) and for the final moisture (VWC<sub>fin</sub>) content. The experiment results' order continued by calculating the mean of results for moisture conditions (initial

and final) for 24 treatments (four sensors and six soil textures) and then viewing the results by tables and histograms.

#### **Traditional calibration method using plant pots**

In the second method of calibration (Figure 4B), plant pots with a volume of 6 l (21.5, 14 cm diameter, and 23 cm height) of known weight earlier prepared for the six soil types had three replications each (18 units). Each container received 4 kg of air-dry soil after calculating its gravimetric water content based on the oven-dry ground representing the hygroscopic content of water for each dirt. Recording the volume of soil inside the container to calculate soil bulk density went on by dividing the soil mass by its amount, then adding 1000 cm<sup>3</sup> to each container of low salt tap water (EC = 0.8 ds/cm) to avoid reading errors in high salt, particularly in resistance sensors (METER, 2020). When the water settled and its movement stopped, soil pots' weight recording followed, with readings taken for each sensor noting it at a temperature not exceeding 35 °C to avoid reading errors on the scale at high temperatures. After subtracting the empty container's weight, continuously noting the wet soil weight occurred. Readings continued recording with the weight of the container every 48 h, for a total of five renderings, to allow for the evaporation of a suitable amount of water and get different

reads. The actual volumetric soil moisture ( $\Theta_{act}$ ) computation employed the following equations:

$$M_w = M_{sw} - M_s \text{ -----(2)}$$

$$V_w = \frac{M_w}{\rho_w} \text{ -----(3)}$$

$$\% \theta_{act} = \frac{V_w}{V_t} \times 100 \text{ -----(4)}$$

Where:

$M_w$  = Mass of water in pot (g)

$M_{sw}$  = Mass of wet soil (g)

$M_s$  = oven dry soil Mass (g)

$V_w$  = volume of water in pot ( $\text{cm}^3$ )

$\rho_w$  = water density ( $\text{g. Cm}^{-3}$ )

$\Theta_{act}$  = actual moisture volumetric ( $\text{cm}^3.\text{cm}^{-3}$ )

$V_t$  = soil volume in pot ( $\text{cm}^3$ )

The experimental design used the factorial system according to the complete randomized design (CRD) with 72 treatments (four sensors, six soil types, and three replicates).

**Data recorded**

Data from the three sensors, i.e., YL-69, SKU: SEN0193, and IC Station, were attainable using the mobile device via the Blynk app (Figure 2) (Lokhande *et al.*, 2022). For the WH51 sensor, the data transmission employed the WS View application, available from smartphones or the ecowitt.net website, as shown in Figure 3.

**Statistical analysis**

After obtaining the data, comprised of sensor readings and their corresponding actual volumetric water content, the said data's statistical processing ran through the Excel application, acquiring the relationship through regression statistics, per the equations shown in Table 4, and some statistical analysis tools with the equations displayed in Table 5. The sum of the coefficients ( $n = 30$ ) for each moisture condition and sensor type included testing all readings for all soils and two moisture conditions (A.S.I.F) and the sensor type with a sum of treatments ( $n = 60$ ). In the second method, 15 samples representing six soil types had three replications for each soil and allergen form, also testing treatments for all soil and sensor types ( $n = 90$ ).

Achieving the probability equation used the calibration equation with the highest determination coefficient ( $R^2$ ). The equations' testing continued by plugging in X-factor the default values of sensor readings (1-100), then extracting predictive values  $\Theta_{pro}$ , which are corresponding sensor reading values, and comparing the predictive values (equation outputs) with the actual  $\Theta_{act}$  values to obtain results of statistical processes. The mean values of statistical results are visible using histogram forms with a Pareto chart, which shows the cumulative ratio of the statistical results. Comparing the results between the first and second methods used the factorial CRD design at two procedures, four sensors, and six soil textures, totaling 48 treatments.

**Table 4.** Regression statistics used in developing the results of the study.

Coefficient of determination (R Square)	$R^2 = 1 - \frac{\sum_i (y - y^{\wedge})^2}{\sum_i (y - \mu)^2}$
Standard Error (S.E.)	$s = \sqrt{\frac{1}{N - 1} \sum_{i=1}^N (x_i - \bar{x})^2}$ ,
Spearman's Rank Correlation Coefficient ( $r_s$ )	$r_s = 1 - \frac{6 \sum D^2}{n(n^2 - 1)}$
Pearson correlation ( $r_p$ )	$r_p = \frac{(\sum x - x') - (\sum y - y')}{\sqrt{[\sum (x - x')^2][\sum (y - y')^2]}}$

**Table 5.** Statistical analysis tools used in research.

Statistic	Equation	
Mean Absolute Deviation (MAD)	$MAD = \frac{\sum_{t=1}^n  A_t - F_t }{n}$	At = actual value Ft= forecast value n = number of observations
Root Mean Square Error (RMSE)	$RMSE = \sqrt{\frac{\sum_{t=1}^n (A_t - F_t)^2}{n}}$	
Mean Absolute Percentage Error (MAPE)	$MAPE = \frac{\sum_{t=1}^n \left  \frac{A_t - F_t}{A_t} \right }{n} \times 100$	

## RESULTS AND DISCUSSION

### Laboratory calibration of repacked soils method

By processing the sensor reading results with  $\Theta_{act}$ , calibration results showed that linear and exponential equations are the best in correlation; thus, choosing them to test accuracy. All calibration equations in the WH51 sensor are linear, while most are exponential in low-cost sensors due to a limitation in their reading range.

The moderate-cost WH51 sensor showed the lowest standard error, while the low-cost IC Station sensor had the highest due to the limiting reading range (<15%  $\Theta$ ), corresponding with the findings of Batllori (2020). In soils, SE ranged between 9.43 and 15.21, with GHB sandy clay loam, DSJ sandy loam, and AGB clay loam showing lower SEs. However, the FGHB sandy loam soil had a higher SE at 61% than the lower GHB (9.43). These results were far from the findings of Varble and Chávez (2011), who reported that the errors were broader in the soil with a higher clay content for all sensors. It might be due to the decrease in error at the final moisture condition, which provided greater homogeneity in the moisture spread, thus reducing the error when measuring the sensor. However, the analysis showed no significant differences among the treatments and the coefficient (36.7%) of difference for the standard error values between the initial and final wet conditions.

Spearman's correlation (rs) results showed average values ranging between 0.79 as a minimum and 0.95 as a maximum, with a coefficient of difference (3%) between sectors. It indicates that the trend of the sensor readings was positive for all types of sensors and soils. It was also notable that the lowest value of Spearman's correlation was by treating all soils with A.S. (0.79), which was foreseeable with the increase in the total number of treatments in this test, and the texture of soils differed in their water characteristics. However, these results considerably have a better correlation and a positive trend, not contrary from previous findings (Adla *et al.*, 2020). The Pearson Correlation (rp) was almost identical to Spearman's Correlation (rs), which confirms the strength of the relationship and the positive trend between sensor readings and actual soil moisture, not only for one type of soil but for all soil types used in the study. Compared with the Pearson correlation coefficient, the Spearman correlation coefficient operates on the ranks of the data rather than on the raw data, and it does not require a relationship between variables. Spearman correlation coefficient is insensitive to extreme data, and in this case, this property would become a disadvantage since the performance of sensors in extreme situations is a concern (Ye *et al.*, 2015).

The low-cost sensors did not show a strong R<sup>2</sup> correlation coefficient in the calibration equations (on average 0.55–0.65), while the moderate-cost sensor WH51 had an

average correlation coefficient of 0.8. These results are not identical with Adla *et al.* (2020), which has a higher  $R^2$  coefficient of determination. The correlation strength between the sensor reading and  $\Theta_{act}$  reflected the difference in the sensor reading between the initial and final moisture status and the difference between soils in their water properties. These results got confirmation from past findings wherein they reported that a sensor behaves differently depending on the soil type's location, and with the same  $\Theta$ , it reads a different signal for each soil (Batllori, 2020). The sensitizers and soil types differed through error analysis after comparing the outputs of the equations with the actual moisture content. Therefore, the GHB-sandy clay loam soil showed a relatively low MAD and RMSE. As for MAPE %, DSJ-loam sandy desert soils showed low in all sensor types due to a better moisture distribution in medium-textured soils (Adla *et al.*, 2020).

#### **Traditional calibration method using plant pots**

The sensor WH51 showed superiority in the R square, rs, and RP values, similar to the results in the first method, which confirms the efficiency of the capacitive average-cost sensor over other low-cost sensors (Adla *et al.*, 2020; Batllori, 2020). The two sensors, i.e., SEN0193 and IC Station, recorded lower values of rs and rp and a decrease in the  $R^2$  (0.69 and 0.57, respectively). The result indicates that the sensors' readings have a positive trend with the actual moisture; however, the variation in the appraisals was not proportional to the changes in the actual moisture values. A similarity was evident in the scores of w, rs, and rp among all types of soils, with an average that did not fall below 0.87, while the average values of  $R^2$  ranged from 0.68 to 0.84. RSJ sandy loam soil recorded a higher value for Sr and rp, while AGB clay loam soil had the lowest. These results support previous findings that the soil with a higher clay content has huge errors (Varble and Chávez, 2011).

Clay loam soil (AGB) with treatment (A.S) represents all types of soils, with the lowest value of  $R^2$ . However, these results

correspond with the first method with AGB down regression ( $R^2 = 0.65$ ). Table 6 shows there was a decrease in the average  $R^2$  values of the sensor IC Station with all types of soils, with an average of 0.69, probably because it works in a low range of moisture (0%–15%), as indicated by Batllori (2020), who reported that the IC Station has a lower influence on soil type. The standard error values ranged from 1.05 to 8.74, lower than the first method, and the order of the sensors was from lowest to highest, i.e., WH51 < YL69 < SEN0193 < IC Station, while the order of the types of soils, i.e., DSJ < BGHB < RSJ < AGB < GHB < FGHB < A.S, was from lowest to highest. The result corresponds with the order of  $R^2$  for the same reasons.

In Table 7, the mean absolute deviation (MAD) and root-mean-square error (RMSE) were the lowest for the capacitive sensor WH51, with a significant difference from the resistive sensor IC Station of 2.2 and 2.59 times at a significance ( $P < 0.05$ ) according to statistical analysis. The average absolute error percentage (MAPE %) values, which were the same among the sensors, ranged from 22.27 in SKU: SEN0193 to 26.45 in WH51, which is a good percentage for error. All types of soils significantly differed in their response to the sensors, where L.S.D was 0.528, 0.6359, and 5.544 for MAD, RMSE, and MAPE%, respectively. The lowest percentage of MAD and RMSE was in BGHB-sandy clay loam and DSJ-sandy loam soils, with an average MAD of 2.41 and 2.5 and RMSE of 3.04 and 2.89, respectively. The riverine RSJ-sandy clay loam soil was evident with the highest values of 3.72 and 5.04, respectively, with no relationship between clay, sand, and organic matter rates with error analysis parameters, which may be due to no high difference between soil types on these properties (Table 3). The results of MAPE % did not differ in this context and ranged between 12.37% DSJ (Sandy Loam) to 35.02% RSJ (Sandy Loam) as the highest MAPE%. From Table 7, however, the lowest values of the MAD and RMSE error analysis were apparent with RSJ-soil using the sensor WH51, except for the RMSE value, which was lower at the DSJ-soil using the sensor WH51. The results are not different after testing 15 reads

**Table 6.** Calibration equations and coefficient of determination R<sup>2</sup> for the experimental treatments in the second calibration method after taking the relationship between all sensor readings for each soil type (15 readings) and all sensor readings for all soils (90 readings), represented by the symbol A.S.

Method 2	Very Low cost		Low cost	
Sensor	YL69		SKU: SEN0193	
Soil	Model equation	R <sup>2</sup>	Model equation	R <sup>2</sup>
AGB	y = 1.8982e0.035x	0.85	y = 0.5335e0.0604x	0.87
FGHB	y = 1.9592e0.0313x	0.93	y = 0.5422e0.0562x	0.71
GHB	y = 1.5108e0.0323x	0.87	y = 0.3593e0.0597x	0.83
BGHB	y = 1.5665e0.0333x	0.94	y = 0.2e0.0711x	0.96
DSJ	y = 8.3646e0.0151x	0.92	y = 5.4333e0.0259x	0.87
RSJ	y = 1.4072e0.0324x	0.83	y = 0.4333e0.0571x	0.71
A.S.	y = 2.2271e0.0295x	0.81	y = 0.7564e0.0514x	0.69
Average		0.88		0.81
	Low cost		Moderate cost	
Sensor	ICStation		WH51	
Soil	Model equation	R <sup>2</sup>	Model equation	R <sup>2</sup>
AGB	y = 2.0825e0.0272x	0.57	y = 0.448x + 0.26	0.87
FGHB	y = 1.861e0.0275x	0.54	y = 0.7439x - 7.0468	0.98
GHB	y = 1.2774e0.0314x	0.79	y = 0.6194x - 5.4378	0.97
BGHB	y = 0.9676e0.0341x	0.80	y = 0.5521x - 4.1865	0.94
DSJ	y = 7.6485e0.0141x	0.82	y = 0.7522x - 0.9115	0.99
RSJ	y = 1.0057e0.0316x	0.69	y = 0.8403x - 12.745	0.98
A.S.	y = 1.8467e0.0276x	0.64	y = 20.254ln(x) - 51.951	0.86
Average		0.69		0.94

in error analysis parameters. Generally, the sensors work well, and the same with the coarse and medium soils for other sensors (Adla *et al.*, 2020; Batllori, 2020; Placidi *et al.*, 2020), with the values of MAD and RMSE for resistant and capacitive sensors were in analogy with previous findings (Kinzli *et al.*, 2012; Adla *et al.*, 2020).

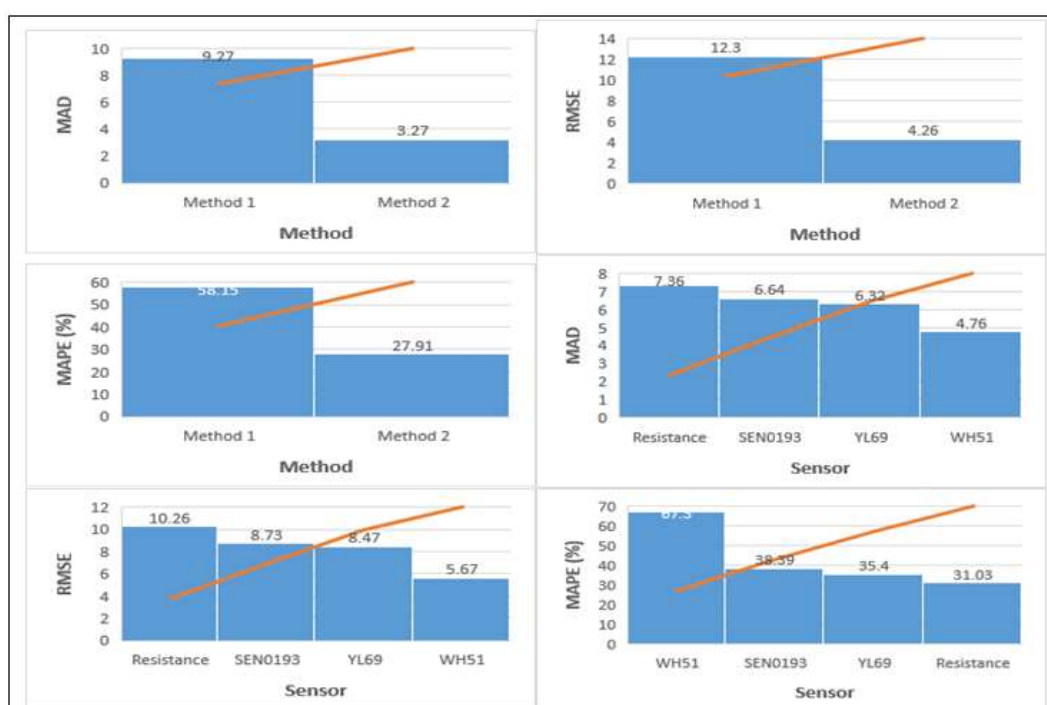
The calibration equations with the highest coefficient of R<sup>2</sup> determination gained preference, with Table 6 showing the equations for the moderate cost sensor WH51 as of the first degree, and this corresponds to the manufacturer's model (Ecowitt, 2022a). The exponential function equations showed the most suitable for the rest of the low-cost sensors due to their limited working range with soil moisture (Batllori, 2020). It turns out that the coefficient of determination of the equations for all types of soils was good for the sensors WH51 and YL69 and average for the sensors resistive IC Station and SEN019. It might be due to the low performance of both sensors in some soils that have clay as AGB - clay loam and in the high range of soil moisture (Batllori, 2020), as well as might be

due to the effect of salts and temperature for the first method (METER, 2020). The standard error for the second method revealed the highest in the mentioned soils.

Calibration equations' testing ran for all the replications of soil type (15 readings representing five moisture levels for three replicates). Table 6 shows the ranking of mean R<sup>2</sup> as WH51 > YL69 > SEN0193 > IC Station. The mean values of MAD and RMSE were YL69 > SEN0193 > IC Station > WH51. The average MAPE% has few differences between sensors, ranging from 24.17 to 27.4, and soils vary in their response to the sensors (Table 7). The highest average values of MAPE% appeared in AGB-clay loam, BGHB-Sandy clay loam, and RSJ-sandy loam, with average percentages not exceeding 35.02% in RSJ. But, an increase in MAPE% emerged for AGB and BGHB soils using the sensor WH51 (54.71% and 53.63%, respectively). It also confirms that the sensor WH51 works better with grounds with a lower percentage of clay, such as river and desert soils, unlike other sensors that recorded the highest MAPE% in riverain soil (RSJ). In general, the average MAPE was 25.54%, which

**Table 7.** The values of the error analysis tool for the experimental treatments of the second method using 15 test representing 3 replicates and 5 moisture stages for each sensor (average without A.S.).

Sensor	Parameter / Soil	AGB	FGHB	GHB	BGHB	DSJ	RSJ	A.S.	Average
	N	15	15	15	15	15	15	90	15
WH51	MAD	2.90	0.93	1.26	1.67	0.88	0.67	3.31	1.38
	RMSE	3.41	1.17	1.43	2.03	1.04	0.72	4.01	1.63
	MAPE (%)	53.64	12.08	24.82	47.66	6.23	14.28	47.12	26.45
YL69	MAD	2.61	2.30	3.00	2.66	2.34	3.78	3.85	2.78
	RMSE	3.41	2.69	3.56	3.39	2.66	4.93	4.89	3.44
	MAPE (%)	15.10	18.14	23.85	34.87	11.29	37.16	38.28	23.40
IC Station	MAD	4.55	5.85	3.33	3.45	3.67	5.87	5.25	4.45
	RMSE	6.16	7.46	4.94	4.47	4.43	7.74	6.73	5.86
	MAPE (%)	24.28	32.81	18.18	20.32	16.62	45.12	40.05	26.22
SEN0193	MAD	2.91	4.03	3.29	1.87	3.11	4.56	4.90	3.29
	RMSE	3.76	5.67	4.69	2.28	3.45	6.77	6.16	4.44
	MAPE (%)	25.50	21.59	19.33	12.37	15.34	39.50	43.02	22.27
Average	MAD	3.24	3.28	2.72	2.41	2.50	3.72	4.33	2.98
	RMSE	4.18	4.25	3.66	3.04	2.89	5.04	5.45	3.84
	MAPE (%)	29.63	21.16	21.55	28.81	12.37	34.02	42.12	24.59



means that the validity of the measurement for these types of inexpensive sensors reaches approximately 75% or more, indicating that these sensors were suitable for use in the prevailing soils of the region. The accuracy of the sensor WH51 was close to that reported by the company (Ecowitt, 2022a), with an average MAE (1.62%) for all types of soils

(Table 7). These results agree with the findings of Adla *et al.* (2020), where the sensor YL69 provided lower error values, and the sensor SEN0193 provided similar values to the capacitive sensors, such as WH51, which confirmed the findings of Batllori (2020) and Placidi *et al.* (2020) that accuracy in it was still higher.

Figure 5 shows that the traditional calibration method recorded the lowest average error analysis compared with the first method. The percentage differences for MAD, RMSE, and MAPE % between the two approaches were 1.89, 1.83, and 1.08 times, respectively. The reason might be that there was just one addition in the second method, with readings recorded for five moisture stages during evaporation. In contrast, in the first method, five levels of added moisture came from two moisture stages (initial and final). There were many readings of the soil moisture levels to reach the most accurate equation, in addition to the first method, designed for calibration with a high-cost precise device, Theta Probe, which was inaccessible. The average error analysis values of the second method were also good for adopting the calibration equations. The MAD average values for all types of sensors for the two methods ranged from 4.76% to 7.36%. These results were acceptable, especially for low-cost

sensors, as per previous calibration (Kinzli *et al.*, 2012; Adla *et al.*, 2020) and manufacturer's calibration of some sensors, such as SM100 and SMEC300 (Spectrum, 2014; Spectrum, 2015), confirming the possibility of using low-cost technologies for monitoring environmental variables as motioned by Schwamback *et al.* (2023), as compared with previous researches.

After adopting the calibration equations for the second method (Table 6), the obtained assumed readings of the moisture limits for each type of experimental soil are in Table 3. Reading limits (Table 8) for the range of available water ( $\Theta_{fc}$  to  $\Theta_{w.p}$ ) lie between 50%–80%, 50%–65%, 60%–95%, and 25%–40% for YL69, SKU: SEN0193, ICStation, and WH51, respectively, by the equation of all soil (A.S), while soil, such as RSJ sandy loam has limits at 35%–80%, 40%–70%, 45%–95%, and 20%–40%, respectively, and AGB clay loam 55%–80%, 50%–70%, 65%–100%, and 25%–75%, respectively.

**Table 8.** The default readings of the sensors and the corresponding volumetric water content ( $\Theta$ ), by applying calibration equations for the second method on each type of soil (\*pointing to down or over range of  $\Theta$ ).

Sensor	Very Low cost - YL69					Low cost - SKU: SEN0193				
	$\Theta$ cm.m <sup>-1</sup>					$\Theta$ cm.m <sup>-1</sup>				
Read value	100	75	50	25	5	83	75	50	25	5
AGB	62.86	26.20	10.92	4.55	2.26	80.23	49.49	10.93	2.42	0.72
BGHB	44.81	20.49	9.37	4.28	2.29	57.54	36.70	9.01	2.21	0.72
GHB	38.19	17.03	7.60	3.39	1.78	50.98	31.62	7.11	1.60	0.48
FGHB .	43.77	19.04	8.28	3.60	1.85	73.10	41.39	7.00	1.18	0.29
DSJ	37.86	25.96	17.80	12.20	9.02	46.63	37.90	19.84	10.38	6.18
RSJ	35.93	15.98	7.11	3.16	1.65	49.55	31.38	7.53	1.81	0.58
A.S	42.55	20.35	9.73	4.66	2.58	53.89	35.72	9.88	2.73	0.98
Sensor	Low Cost - ICStation					Moderate Cost - WH51				
	$\Theta$ cm.m <sup>-1</sup>					$\Theta$ cm.m <sup>-1</sup>				
Read value	100	75	50	25	5	100	75	50	25	15
AGB	31.61	16.02	8.11	4.11	2.39	45.06	33.86	22.66	11.46	6.98
BGHB	29.11	14.64	7.36	3.70	2.14	67.34	48.75	30.15	11.55	4.11
GHB	29.51	13.46	6.14	2.80	1.49	56.50	41.02	25.53	10.05	3.85
FGHB .	29.28	12.49	5.32	2.27	1.15	51.02	37.22	23.42	9.62	4.10
DSJ	31.33	22.02	15.48	10.88	8.21	74.31	55.50	36.70	17.89	10.37
RSJ	23.70	10.76	4.88	2.22	1.18	71.29	50.28	29.27	8.26	down
A.S	29.18	14.63	7.34	3.68	2.12	41.32	35.50	27.28	13.24	2.90

**Table 9.** Assumed values of moisture sensor readings for volumetric moisture content at saturation, field capacity, after depletion of 55% of the available water, and at the permanent wilting point

	Moisture Limits				Read				
	Soil Type	$\Theta$ cm.m <sup>-1</sup>	YL69	SKU: SEN0193	IC Station	WH51	Max	Aver	Min
Field Capacity	AGB	36.50	84	70	100	80	100	84	70
	FGHB	13.59	62	57	72	28	72	55	28
	GHB	15.70	72	63	79	34	79	62	34
	BGHB	17.39	72	63	85	39	85	65	39
	DSJ	36.11	97	73	100	49	100	80	49
Depletion 50%	RSJ	10.30	51	55	62	27	62	49	27
	AGB	24.55	73	63	91	54	91	70	54
	FGHB	11.79	57	55	67	25	67	51	25
	GHB	11.95	64	58	71	28	71	55	28
	BGHB	13.99	65	60	78	33	78	59	33
Wilting Point	DSJ	26.94	78	62	89	47	89	69	47
	RSJ	7.35	40	44	50	19	50	38	19
	AGB	12.60	54	52	66	27	66	50	27
	FGHB	9.99	52	52	60	23	60	47	23
	GHB	8.20	52	52	60	22	60	47	22
Max Fc.	BGHB	10.59	57	56	70	27	70	53	27
	DSJ	17.76	49	45	60	25	60	45	25
	RSJ	4.40	35	34	31	20	35	30	20
Max Dep.			97	73	100	80	100	88	73
Max. W.p.			78	63	91	54	91	72	54
			57	56	70	27	70	53	27

In general, most crops experience stress when the soil available water depletion is 30%–50% (Sharma, 2019). Hence, what concerns us in the irrigation field is the range of the sensor reading between the field capacity and when 50% of the available water, which ranges between depletion and permanent wilting point, gets depleted. For example, Table 9 shows that the reading range between  $\Theta_{f.c}$  to  $\Theta_{w.p}$  according to the second method equations in the sensor WH51 for AGB soil was 80–27, and the same is the maximum range in all soils, while in the sensor YL69, the said range was 84–54 for the same ground, with a the utmost extent of 97–57 for all soils. The maximum scopes of the readings between  $\Theta_{f.c}$  to  $\Theta_{w.p}$  in all soil (100–70) is the same in the IC station sensor due to its limited reading range (Batllori, 2020), which, in such a case, has referred to the average for maximum depletion value showing that the sensor reading reaching the limits of 72 ( $\pm 2$ ) adopt 3% MAD for all sensors (Table 7). However, IC station sensor is better only in sandy soil, giving a reading indicating that more than 50% of the available water has disappeared,

requiring immediate irrigation without delay. Therefore, the expectation of the lowest possible moisture level falls within the extent of depletion, where the general mean of the RMSE was 4%, and MAPE was 25% (Table 7). It means that the measurement accuracy for sensors reaches 75% or even more.

## CONCLUSIONS

It is noteworthy that the sensors provide accuracy and speed of measurement, reducing effort and time with the more measurement tests carried out, the more accurate and less error results attained. Overall, the low-cost sensors perform relatively well and can be helpful in soils that do not suffer from salinity problems; however, make sure not to take the readings at extreme temperatures. The sensor calibration can be according to its equations for each soil type. Tests on allergens have not continued in saline soils; therefore, further studies require consideration to know the effect of soil salinity conditions and temperature on the performance accuracy of

soil moisture sensors. Based on these results, we can say that moderate-cost sensors have good accuracy, and low-cost sensors have suitable accuracy. Some, however, such as the IC station, have limited use for some soils, especially those with a high range of available water, i.e., clay and sandy loam desert soils that respond well to the other sensors.

## REFERENCES

- Abbas KN (2021). The effect of natural factors on the cultivation and production of sesame crop in Al-Qadisiyah Governorate. *J. Coll. Educ. Women* 32(2): 131-146. <https://doi.org/10.36231/coedw.v32i2.1496>.
- Adla S, Rai NK, Karumanchi SH, Tripathi S, Disse M, Pande S (2020). Laboratory calibration and performance evaluation of low-cost capacitive and very low-cost resistive soil moisture sensors. *Sensors J.* 20(2): 363. <https://www.mdpi.com/1424-8220/20/2/363>.
- Adla S, Rai N, Harsha KS, Tripathi S, Disse M, Pande S (2019). Laboratory calibration of soil moisture sensors in porous media (repacked soils). Available online: <https://www.protocols.io/view/laboratory-calibration-of-soil-moisture-sensors-in-x54v9xjmv3eq/v2?step=6>.
- Adnan F (2018). Arduino World. AL-Rafid Publications. <https://www.facebook.com/bookfarkadnan/posts/294158254607082>.
- Afifie NA, Khang AW, Amin AF, Alsayaydeh JA, Indra WA, Herawan SG, Ramli AB (2021). Evaluation method of mesh protocol over ESP32 and ESP8266. *Baghdad Sci. J.* 18(4): 1397-1405. doi: [https://dx.doi.org/10.21123/bsj.2021.18.4\(Suppl.\).1397](https://dx.doi.org/10.21123/bsj.2021.18.4(Suppl.).1397).
- Ahmad FH, Jber AS, Salman AD (2006). Effect of phosphate fertilizer, soil texture and irrigation water source on some chemical properties of soil. *Iraqi J. Agric. Sci.* 37(3): 13-20.
- Al-Halfi DA, Al-Azzawi SS (2022). Effect of organic fertilizer sources and chemical fertilization on some soil physical traits and yield of summer squash (*Cucurbita pepo* L.). *Iraqi J. Market Res. Consum. Prot.* 14(2): 74-81. [http://dx.doi.org/10.28936/jmracpc14.2.2022.\(9\)](http://dx.doi.org/10.28936/jmracpc14.2.2022.(9)).
- Al-Lami AA, Al-Rawi SS, Ati AS (2023). Evaluation of the aquacrop model performance and the impact of future climate changes on potato production under different soil management systems. *Iraqi J. Agric. Sci.* 54(1): 253-267. <https://doi.org/10.36103/ijas.v54i1.1698>.
- Al-Mafrajee WM, El-Rubae FA (2022). Effect of spraying organic emulsion (Appetizer) and nano npk with urea on some growth characteristics of three synthetic cultivars of maize. *Iraqi J. Market Res. Consum. Prot.* 14(1): 108-117. [http://dx.doi.org/10.28936/jmracpc14.1.2022.\(12\)](http://dx.doi.org/10.28936/jmracpc14.1.2022.(12)).
- Al-Rawi MA (2014). The impact of cultivation and soil surface slope on some physical and chemical properties of Al-Obeidi oasis soil - Western desert - Iraq. Master Thesis. Agric. Coll. Univ. of Baghdad.
- Al-Rawi MA (2017). Evaluation state of degradation of tillage and non-tillage agricultural by adopting the stability indicator of dry aggregates in province of Baghdad - Iraq. *J. Agric. Vet. Sci.* 10(8): 16-19. <https://doi.org/10.9790/2380-1008031619>.
- Al-Rawi MA, Al-Mashhadani DI (2021). The response of growth of some lawn plants to chemical fertilization with humic acid under low-light conditions of house garden. *Plant Arch. J.* 21(1): 1212-1218. <https://doi.org/https://doi.org/10.51470/PLANTARCHIVES.2021.v21.S1.191>.
- AL-Rawi MA, Bahia, M. H. S. (2020). Study of water productivity for wheat and barley crops in some irrigated region in Iraq. 10th Int. Conf. Sustainable Agric. Dev. 2-4 March 2020. *Fayoum J. Agric. Res. Dev.* 34(1(B): 272-287. [www.fayoum.edu.eg/Agri/conference10/pdf/3.pdf](http://www.fayoum.edu.eg/Agri/conference10/pdf/3.pdf).
- Batlloori GN (2020). Development and testing of hygrometers with Arduino low-cost electronic components. Master Thesis [Politecnico Di Torino]. <https://upcommons.upc.edu/handle/2117/333706>.
- Bishay FK (2003). Towards sustainable agricultural development in Iraq. The transition from relief, rehabilitation and reconstruction to development. *Food Agric. Organ. United Nations (FAO)* Rome. <https://www.fao.org/3/Y9870E/y9870e00.htm>.
- Bittelli M, Salvatorelli F, Pisa PR (2008). Correction of TDR-based soil water content measurements in conductive soils. *Geoderma J.* 143(1-2): 133-142. <https://doi.org/10.1016/j.geoderma.2007.10.022>.
- Buringh P (1960). Soils and soil conditions in Iraq. Republic of Iraq. Ministry of Agric. Directorate Gen. Agric. Res. Projects.
- Buringh P, Edelman CH (1955). Some remarks about the soils of the alluvial plain of Iraq, South

- of Baghdad. *Netherland J. Agric. Sci.* 3(1): 40-49.
- Campbell CS, Campbell GS, Cobos DR, Bissey LL (2009). Calibration and evaluation of an improved low-cost soil moisture sensor. Decagon Devices. Available online: <https://www.irrigation.org/IA/FileUploads/IA/Resourad/TechnicalPapers/2007/CalibrationAndEvaluationOfAnImprovedLow-CostSoilMoistureSensor.pdf>.
- Campbell CS, Cobos DR, Bissey LL (2007). Calibration and Evaluation of an Improved Low-Cost Soil Moisture Sensor. Application Note 800-755-2751; Decagon Devices, Inc.: Pullman, WA, USA. p. 13.
- Ecowitt (2022a) WH51 Wireless soil moisture sensor max 8 channels soil humidity tester. Retrieved from: <https://www.ecowitt.com/shop/goodsDetail/19>. September 24, 2022.
- Ecowitt (2022b). <https://www.ecowitt.net/home/index?id=84837>. September 24 (2022).
- Eltaiif NI, Gharaibeh MA (2022). Soil erosion catastrophe in Iraq-Preview, Causes and Study Cases. *Environ. Degrad. Asia: Land Degrad. Environ. Contam. Hum. Act.* pp. 179-207. [https://doi.org/10.1007/978-3-031-12112-8\\_9](https://doi.org/10.1007/978-3-031-12112-8_9).
- IC Station (2022). Soil moisture hygrometer detection humidity sensor module corrosion resistance probe dc 3.3-12v for Arduino. Retrieved from: <https://www.icstation.com/soil-moisture-hygrometer-detection-humidity-sensor-module-corrosion-resistance-probe-arduino-p-12322.html>. September 24, 2022.
- Isa HA, Suliman AA (2020). The relationship between reflectivity and some physical properties of desert soils using geospatial techniques and spectroradiometer in Najaf Governorate of Iraq. *Plant Arch.* 20(1): 1657-1665.
- Jackson CR (1992). Hillslope infiltration and lateral downslope unsaturated flow. *J. Water Resour. Res.* 28(9): 2533-2539.
- Kagalkar A (2017). Smart irrigation system. *Int. J. Eng. Res. Technol.* 6(5): 982-986.
- Kinzli KD, Manana N, Oad R (2012). Comparison of laboratory and field calibration of a soil-moisture capacitance probe for various soils. *Journal of Irrigation and Drainage Engineering.* Apr 1:138(4):310-21. [https://doi.org/10.1061/\(ASCE\)IR.1943-4774.0000418](https://doi.org/10.1061/(ASCE)IR.1943-4774.0000418).
- Kukal Z, Al-Jassim J (1971). Sedimentology of pliocene molasse sediments of the Mesopotamian geosyncline. *Sediment. Geol.* 5(1): 57-81. [https://doi.org/10.1016/0037-0738\(71\)90019-4](https://doi.org/10.1016/0037-0738(71)90019-4).
- Lokhande LR, Kale MA, Shinde SS (2022). Fault detection and monitoring hybrid power plant by using IOT. *Int. Res. J. Modernization in Eng. Tech. Sci.* 4(6). [www.irjmets.com](http://www.irjmets.com).
- Mander G, Arora M (2014). Design of capacitive sensor for monitoring moisture content of soil and analysis of analog voltage with variability in moisture. *Recent Adv. Eng. Comput. Sci.* 1-5. doi: 10.1109/RAECS.2014.6799646.
- METER G (2020). «Soil moisture sensors - How they work. Why some are not research-grade». In: (July 2020) (cit. on pp. 5, 30, 38). <https://www.metergroup.com/en/meter-environment/measurement-insights/tdr-fdr-capacitance-compared>.
- Muhaimeed AS, Al-Falihi AA, Al-Aini E, Taha AM (2014). Developing land suitability maps for some crops in Abu-Ghraib using remote sensing and GIS. *Remote Sens. GIS* 2: 16-23.
- Muhaimeed AS, Muhammad A (2010). Study the nature of mineral composition for some soil series of river levees in Iraqi alluvial plain. *Tech. J.* 23(2): 65-80.
- Muzdrikah FS, Nuha MS, Rizqi FA (2018). Calibration of capacitive soil moisture sensor (SKU: SEN0193). 2018 4th Int. Conf. Sci. Tech. pp. 1-6. <https://doi.org/10.1109/ICSTC.2018.8528624>.
- Placidi P, Gasperini L, Grassi A, Cecconi M, Scorzoni A (2020). Characterization of low-cost capacitive soil moisture sensors for IoT networks. *Sensors.* 20 (12):3585. <https://doi.org/10.3390/s20123585>.
- Salman AA, Alisa ZT (2019). Improving the network lifetime in wireless sensor network for internet of thing applications. *Al-Khwarizmi Eng. J.* 15(4): 79-90. <https://doi.org/10.22153/kej.2019.09.007>.
- Schwamback D, Persson M, Berndtsson R, Bertotto LE, Kobayashi AN, Wendland EC (2023). Automated low-cost soil moisture sensors: Trade-off between cost and accuracy. *Sensors.* Feb 22;23(5):2451. <https://doi.org/10.3390/s23052451>.
- Setyowati I, Novianto D, Purnomo E (2020). Preliminary design and soil moisture sensor y1-69 calibration for implementation of smart irrigation. *J. Phys: Conf. Ser.* 1517(1): 012078.
- Sharma V (2019). Soil moisture sensors for irrigation scheduling. <https://extension.umn.edu/irrigation/soil-moisture-sensors-irrigation-scheduling>. Reviewed in 2019.
- Shenzhen (2022). <https://manuals.plus/shenzhen-fine-offset-electronics-co/gw2000-weather->

- station-manual?expand\_article=1#axzz8Gn6G2Zzs.
- Solijonov K, Umarov FU (2022). Ecology of leeches and gastropods of the lower Ak-buura River, Fergana valley, Uzbekistan. *Bull. Iraq Nat. Hist. Mus.* (P-ISSN: 1017-8678. E-ISSN: 2311-9799). 17(2): 229–250. <https://doi.org/10.26842/binhm.7.2022.17.2.0229>.
- Spectrum Tech. (2014). Waterscout SM100 Soil Moisture Sensor Product Manual. Spectrum Technologies, Inc.:Plainfield, IL, USA, 2014. Available online: [https://www.specmeters.com/assets/1/22/6460\\_SM1002.pdf](https://www.specmeters.com/assets/1/22/6460_SM1002.pdf) July 16 (2022).
- Spectrum Tech. (2015). Waterscout SMEC 300 Soil Moisture Sensor Product Manual. Spectrum Technologies, Inc.: Aurora, IL, USA, 2015. Available online: [https://www.specmeters.com/assets/1/22/6470\\_SMEC3004.pdf](https://www.specmeters.com/assets/1/22/6470_SMEC3004.pdf) July 16 (2022).
- Tutorials RN (2017). Guide for soil moisture sensor yl-69 or hl-69 with Arduino. Retrieved from: <https://randomnerdtutorials.com/guide-for-soil-moisture-sensor-yl-69-or-hl-69-with-the-arduino> September 20, 2022.
- USDA (1975). Soil taxonomy: A basic system of soil classification for making and interpreting soil surveys. Soil Surv. Staff. Coord. Soil Conserv. Serv. Agric. Handb. 436. US Department Agric. (USDA).
- Van der AAM (2003). Classification of mineral water types and comparison with drinking water standards. *Environmental geology*, 44(5), 554-563. <https://doi.org/10.1007/s00254-003-0791-4>.
- Varble JL, Chávez JL (2011). Performance evaluation and calibration of soil water content and potential sensors for agricultural soils in eastern Colorado. *Agricultural water management*. Dec 1;101(1):93-106. <https://doi.org/10.1016/j.agwat.2011.09.007>.
- Ye J, Xiao C, Esteves RM, Rong C (2015). Time series similarity evaluation based on Spearman's correlation coefficients and distance measures. In *Cloud Computing and Big Data: Second International Conference. CloudCom-Asia*. Huangshan. China. June 17-19, 2015, Revised Selected Papers 2 (pp. 319-331). Springer International Publishing. [https://doi.org/10.1007/978-3-319-28430-9\\_24](https://doi.org/10.1007/978-3-319-28430-9_24).